

November 8, 2000

To be submitted to Concrete Science and Engineering

The relationship between the formation factor and the diffusion coefficient of porous materials saturated with concentrated electrolytes: Theoretical and experimental considerations

K.A. Snyder
Building Materials Division
NIST

Abstract:

It has been proposed previously that the formation factor, in conjunction with the self-diffusion coefficient, can be used to determine the apparent diffusion coefficient. Strictly speaking, this application is incorrect. The formation factor is equal to the ratio of the self-diffusion coefficient to the *microstructural* diffusion coefficient, which is a quantity that characterizes the pore structure and is independent of the pore solution electro-chemistry. The origin of this relationship will be shown using both the electro-diffusion transport equation and the definition of the formation factor. In practice, service life models that solve the electro-diffusion transport equation as a function of time require the formation factor in order to calculate the *microstructural* diffusion coefficient; the effects of the pore solution chemistry are then calculated independently. To use such service life models, a method is needed to estimate the formation factor from diffusion data in order to apply the service life model to a particular material. An experiment on a model porous material is used to demonstrate one method for determining the formation factor from divided cell diffusion data. Differences among the self-diffusion coefficients of the various diffusing species accentuates the difference between the microstructural and the apparent diffusion coefficients. The significance of this result to cementitious systems is discussed.

1 Introduction

Electrical measurements hold great promise for estimating the diffusion coefficients of saturated porous materials. The two most commonly used conduction techniques are the electrical migration test (driven diffusion) and the conductivity measurement. Migration tests are used to determine the ionic mobility, which can be related to diffusivity. Conduction tests are used estimate the formation factor, which can also be related to diffusivity. While there have been many reports on the use of the electrical migration tests to determine the diffusion coefficient of cementitious systems [1], there have been fewer reports on the use of the formation factor. This is unfortunate, since the formation factor is directly related to the diffusivity of the material pore structure. However, this relationship between formation factor and diffusivity has subtleties that must be considered when making estimates of one from the other.

The formation factor \mathcal{F} has its origin in geological research on saturated porous materials. For a nonconducting porous solid saturated with a conducting pore solution, the formation factor is the ratio of the pore solution conductivity σ_p to the bulk conductivity σ_b [2]:

$$\mathcal{F} = \frac{\sigma_p}{\sigma_b} \quad (1)$$

This quantity characterizes the solid microstructure since the only difference between the conductivities is due to the restricted pathways through which the current is constrained in the bulk conductivity measurement.

The use of conduction tests to estimate the diffusion coefficient is due to the relationship between conductivity and diffusivity. In an electrolytic solution, the contribution an ionic species makes to the overall conductivity can be expressed as a function of its conventional

(electrochemical) mobility u , amount-of-substance concentration c , and valence z [3]:

$$\sigma = z c F u \quad (2)$$

The quantity F is the Faraday constant. The mobility can then be related to diffusivity through the Einstein relation [3]:

$$zFD = RTu \quad (3)$$

The quantity R is the universal gas constant and T is the absolute temperature. Using these equations, one can estimate the diffusion coefficient from either measurements of ion mobility (driven diffusion) or from the conductivity contribution of a particular ion (conductivity).

Alternatively, if a porous material is saturated with a dilute electrolytic solution, the ratio of the pore solution conductivity σ_p to the bulk conductivity σ_b would be equal to the ratio of the diffusion coefficient of an ion in the pore solution D_p to the bulk diffusion coefficient D_b of that ion:

$$\mathcal{F} = \frac{\sigma_p}{\sigma_b} = \frac{D_p}{D_b} \quad (4)$$

Note that this relationship holds even if the Einstein relation is incorrect at large concentrations; the multiplicative error occurring in both D_p and D_b would cancel. Since the self-diffusion coefficient of ions can be found in books, this is a provocative approach to determining the bulk diffusion coefficient D_b [4].

Unfortunately, the pore solution of typical cementitious systems can have a large ionic strength (0.5 mol·kg⁻¹ to 1.0 mol·kg⁻¹), and so care must be exercised when predicting the bulk diffusion coefficient from the formation factor. At these large ionic strengths the pore solution diffusion coefficient D_p of an ion is different from the self-diffusion coefficient, which is the value reported in tables [5]. Equation 4 can still be used, given that one can correctly determine the diffusion coefficient D_p in the pore solution. However, given the constraints of most experimental diffusion apparatus, and that experimenters typically measure time

dependent concentrations, an exact value for D_p can be difficult to define.

An alternative approach is to determine the formation factor from the diffusion data by separating the microstructural dependence from the concentration dependence in the diffusion coefficient. It will be shown that the formation factor can be alternatively expressed as a function of the *microstructural* diffusion coefficient of the porous material, which is independent of changes in the pore solution chemistry, and the self-diffusion coefficient, which is a quantity that is independent of the diffusion potential. The resulting formation factor could then be used to predict the diffusive transport of any ion within the studied system since it uniquely characterizes the solid pore structure; the chemical effects would be calculated independently.

The origin of the relationship between formation factor and diffusion coefficient will be studied in detail. The analysis will elucidate the proper use of the formation factor for estimating either the microstructural or the concentration dependent diffusion coefficient. Conversely, determining the formation factor from diffusion measurements will also be discussed. The method proposed here will use a computer program to solve the electro-diffusion equation. To demonstrate this method, an experiment was performed on a commercial sintered alumina ceramic specimen, saturated with various electrolytes. The estimate of the formation factor from the diffusion test, after accounting for ion-ion interactions, is compared to the value determined from the conductivity measurement.

2 Theory

The proper application of the formation factor to porous systems containing concentrated electrolytes can be best studied by starting with the appropriate transport equation. For the case of diffusing charged species in concentrated electrolytes, the transport is governed by coupled electrical and diffusive transport, and ion-ion interactions must be also be considered.

2.1 Diffusion Coefficient

The diffusion of ionic species in an electrolyte is governed by the electro-diffusion equation. For the i -th ionic species, the electro-diffusion equation relates the bulk flux \mathbf{j} to the concentration c , the diffusion potential ψ_D , the bulk microstructural diffusion coefficient D_μ , and the bulk conventional mobility u [6]:

$$\mathbf{j} = -D_\mu \left(1 + \frac{\partial \ln \gamma}{\partial \ln c} \right) \nabla c - z F u c \nabla \psi_D \quad (5)$$

The quantity γ is the activity coefficient for the species. Although this equation neglects adsorption effects, it is otherwise a complete description of the nonreacting diffusive transport of charged species in concentrated electrolytes. Equation 5 still bears a resemblance to Fick's law of diffusion [7]. The quantity $D_\mu[1 + \partial \ln \gamma / \partial \ln c]$ is an *agglomerated* diffusion coefficient that includes the effects of changes in both the microstructure and the concentration.

It should be noted that the *agglomerated* diffusion coefficient is not the *apparent* bulk diffusion coefficient D_b . Strictly speaking, the apparent diffusion coefficient also includes the effects of the diffusion potential ψ_D . In those cases where the self-diffusion coefficients of all the diffusing species are nearly identical, the diffusion potential will be nearly zero, and the apparent diffusion coefficient will be nearly equal to the agglomerated diffusion coefficient. However, for cementitious systems, there are many species present with varying self-diffusion coefficients.

Ideally, one would like to distinguish between the effects due to microstructural changes and the effects due to changes in the pore solution electro-chemistry. By observation, one can see that the microstructural diffusion coefficient D_μ characterizes the solid microstructure and that the quantity in parenthesis characterizes the pore solution chemistry. The microstructural diffusion coefficient is itself independent of the pore solution chemistry. Demonstrating how to extract the value of microstructural diffusion coefficient from a diffu-

sion experiment is accomplished through a detailed discussion of the formation factor.

2.2 Formation Factor

Consider an electrical measurement of the formation factor \mathcal{F} performed on a porous specimen saturated with a concentrated electrolyte. The conductivity of the pore solution σ_p is a function of the ionic strength I . The conductivity is proportional to the ionic strength such that as the ionic strength approaches a value of zero, the conductivity also approaches a value of zero. Similarly, the bulk conductivity has the same dependence on the pore solution conductivity. If the pore solution conductivity doubles, the bulk conductivity will also double; surface conduction contributions will be ignored until later in the discussion.

The diffusion coefficient of an ion in a concentrated electrolyte has a different type of dependence on the ionic strength. The self-diffusion coefficients reported in tables are actually in the limit that both the concentration and the diffusion potential go to zero. In the practical dilute limit, the cations and the anions of a 1:1 valence electrolyte must diffuse together due to charge neutrality. This leads to the creation of the diffusion potential. Therefore, the pore solution diffusion coefficient D_p must be an function of the ionic strength, activity coefficients, and the diffusion potential:

$$D_p = D_\infty [1 + g(I, \gamma, \psi_D)] \quad (6)$$

The function g is an arbitrarily complex function of the ionic strength I , the activity coefficient γ , and the diffusion potential ψ_D . The quantity D_∞ is the self-diffusion coefficient that is the value reported in tables. A similar relationship characterizes the bulk diffusion coefficient D_b :

$$D_b = D_\mu [1 + g(I, \gamma, \psi_D)] \quad (7)$$

The microstructural diffusivity D_μ is the corresponding limiting value for the bulk diffusivity.

It is independent of both the activity coefficient and the diffusion potential, and is the same quantity that appears in Eqn. 5.

Using these relations, the formation factor can be written as a function of quantities that are themselves functions of the ionic strength I , activity coefficient γ , and the diffusion potential ψ_D :

$$\mathcal{F} = \frac{\sigma_p(I)}{\sigma_b(I)} = \frac{D_\infty [1 + g(I, \gamma, \psi_D)]}{D_\mu [1 + g(I, \gamma, \psi_D)]} = \frac{D_\infty}{D_\mu} \quad (8)$$

However, the resulting formation factor \mathcal{F} is independent of both the ionic strength and the ionic species; a fact that is exploited by numerical calculations of formation factor on model microstructures [8].

The advantage of using the ratio D_∞/D_μ is not immediately obvious. In Eqn. 4, D_b is observable, but D_p is difficult to determine precisely in typical diffusion apparatus. In Eqn. 8 above, D_∞ can be found in tables, but the quantity D_μ cannot be observed in electrolytes because the effects of the diffusion potential cannot be eliminated. Serendipitously, the usefulness of D_μ in service life prediction through its use in the electro-diffusion equation is also the key to determining this quantity from experiment.

The formation factor is extremely useful in models of ionic transport. Accurate service life predictions will require models that can account for independent changes in either the solid microstructure or the pore solution chemistry. A suitable computer program could solve the electro-diffusion transport equation by using estimates of the ion activity coefficient γ from published empirical relations and using the local electro-neutrality condition to solve for the diffusion potential. The microstructural diffusion coefficient D_μ in the electro-diffusion equation would be calculated from the formation factor \mathcal{F} and the dilute limit self diffusion coefficient D_∞ :

$$D_\mu = \frac{D_\infty}{\mathcal{F}} \quad (9)$$

From this and the boundary conditions, the electro-diffusion equation is completely specified.

Alternatively, one can determine the formation factor from experimental diffusion data by using the same computer program. Using a computer program that implements Eqns. 5 and 9, one adjusts the formation factor until the computed output matches the experimentally observed quantities. The experimental program described subsequently used this approach to determine the formation factor from divided cell diffusion measurements.

3 Experiment

In this experiment, the specimens were a sintered alumina ceramic frit typically used for filtration, with an advertised pore size less than $0.5 \mu\text{m}$. Mercury intrusion porosimetry (MIP) measurements confirmed this value, and also gave an estimated total porosity of 26 %. The cylindrical specimens were 50. mm in diameter and 6.4 mm thick. Each specimen was mounted into an acrylic annulus using an epoxy adhesive. Finally, the mounted specimens were clamped between nearly identical cylindrical glass vessels, with each vessel having a volumetric capacity of approximately 250 mL. The setup for both the conductivity and the diffusion measurements is shown schematically in Fig. 1.

Once the specimens were affixed between the vessels they were placed into an environmental chamber maintained at a temperature of $25 \text{ }^\circ\text{C}$. Both the conductivity and the diffusivity experiments were conducted in this chamber, with all measurements and sampling performed within the chamber.

3.1 Formation Factor

The formation factor measurements were performed using potassium chloride as the pore solution because the conductivity of a few standard solutions are known to a high precision [9]. A range of concentrations were used to ensure that the surface conduction component was properly accounted for. The specimens were first vacuum saturated with a known con-

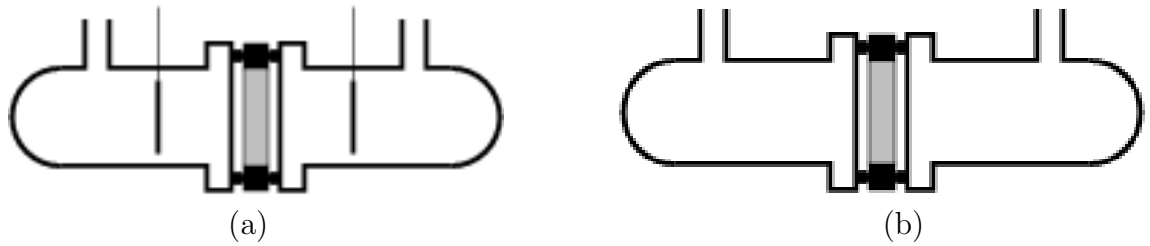


Figure 1: The conductivity cell apparatus(a) and the diffusion divide cell apparatus (b). The schematics depict the configuration of the two cylindrical glass vessels on either side of a mounted specimen. The system is sealed using rubber o-rings; the clamps are not shown. The apparatus differ only in the vertical platinum electrodes in the conductivity cell. The diameter of the specimen, the glass vessels, and the platinum electrodes are approximately 50 mm.

ductivity solution and then mounted, using rubber o-rings and clamps, between two glass vessels, each containing a platinum electrode. The setup is shown schematically in Fig. 1(a). The apparatus, in the absence of a sample and holder, had a conductivity cell constant of 0.3567 cm^{-1} .

To determine the formation factor of the saturated specimen, the cell was filled with the same solution as the saturation solution and then allowed to thermally equilibrate in the environmental chamber. The direct current (dc) resistance of the sample and cell was determined using a commercial impedance spectrometer that sampled frequencies between 10 Hz and 1 MHz. The bulk conductivity of the sample was calculated from the cell constant and the specimen geometry. The formation factor was calculated from the ratio of the known pore solution conductivity to the calculated bulk conductivity.

Pore solution concentrations of $0.01 \text{ mol}\cdot\text{kg}^{-1}$, $0.10 \text{ mol}\cdot\text{kg}^{-1}$, and $1.00 \text{ mol}\cdot\text{kg}^{-1}$ were used to assess the contribution from surface conduction. Due to surface conduction contributions, the formation factor increases with increasing pore solution conductivity, converging to the correct value as the concentration increases. The specimen conductivity measured using the $0.01 \text{ mol}\cdot\text{kg}^{-1}$ solution was approximately 85 % of the value using the $1.0 \text{ mol}\cdot\text{kg}^{-1}$ solution, and the specimen conductivity using the $0.10 \text{ mol}\cdot\text{kg}^{-1}$ solution was approximately 98 % of the value using the $1.0 \text{ mol}\cdot\text{kg}^{-1}$ solution. Therefore, the formation factor calculated

at $1.0 \text{ mol}\cdot\text{kg}^{-1}$ was used as the best estimate. An estimate of the formation factor at infinite conductivity can be estimated from a Padé approximation [10]. Unfortunately, the approximation contains four parameters, and only three conductivity measurements were taken. Nonetheless, the reported result represents a lower bound to the true formation factor. Since the change in formation factor was only 2 % for a ten fold increase in concentration, the true value is probably not more than a fraction of percent larger than the values reported.

Since the ceramic specimens are the result of a controlled commercial process, they have relatively little specimen to specimen variation. The four specimens used in this experiment had formation factors ranging from 10.6 to 10.9. These values were determined after each sample was allowed sufficient time to reach thermal equilibrium, and then the values of the dc resistance varied by less than 1 %. The corresponding calculated formation factor varied by approximately 2 %.

3.2 Diffusion

Upon completion of the conductivity measurements, the specimens were removed from the conductivity cell and saturated with a test solution for use in the divided cell apparatus. The divided cell apparatus was, with the exception of the platinum electrodes, otherwise similar to the conductivity cell. A schematic of the setup is shown in Fig. 1(b).

Four test solutions were chosen for this experiment and are shown in Table 1. The test solution was first used to saturate the specimen and then added to the vessel on one side of the specimen. Potassium iodide was then added to the opposite chamber. The concentration of the potassium iodide was the same as for the test solution.

Transport through the specimen was monitored by periodically measuring the iodide concentration in both vessels as a function of time. For each concentration measurement, a one milliliter sample was taken from each of the two vessels and diluted in water. The iodide concentration was determined using a commercial ion selective iodide combination electrode.

Table 1: Test solutions used in the divided cell experiment. Specimens are initially saturated with the test solution. The opposite vessel contains potassium iodide at the same concentration as the test solution.

Solution	Concentration (mol·L ⁻¹)
KCl	0.1
NaCl	0.1
NaOH	0.1
KCl	1.0

Reference solutions were used to standardize the probe each day the concentrations were recorded. Previous experiments conducted on nearly identical specimens demonstrated that the use of magnetic stirrers has no effect on measured results.

3.3 Analysis

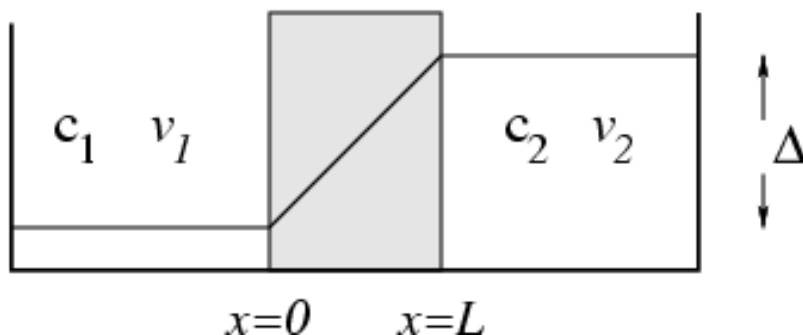


Figure 2: Schematic of the constant gradient hypothesis across a sample with thickness L . Vessels 1 and 2 contain a species with concentrations c_1 and c_2 , and have volumes v_1 and v_2 , respectively.

The analysis of the data can be performed using any one of many possible methods. In this experiment, the concentration of iodide on both sides of the specimen is changing with time. Rather than try to “fit” the time-dependent concentration data on both sides of the cell, the analysis was based upon the difference in concentration between the vessels.

For a sufficiently low diffusivity sample and sufficiently large vessels, the concentration profile across the specimen should become virtually linear after some initial induction pe-

riod. At this point the flux of iodide is constant across the sample, and the corresponding concentration gradient is constant. The schematic shown in Fig. 2 depicts a system in the constant gradient state. The thin line depicts the concentration of iodide throughout the system; constant in each vessel and a straight line with constant slope across the sample. The specimen bulk diffusivity is D_b , the thickness is L , the area is A , and the volume of each vessel is v_1 and v_2 , each with concentration c_1 and c_2 , respectively. Since the flux is constant, the rate of change in iodide concentration in each vessel is also a constant:

$$\frac{\partial c_1}{\partial t} = \frac{AD_b}{v_1} \frac{c_2 - c_1}{L} = \frac{-v_2}{v_1} \frac{\partial c_2}{\partial t} \quad (10)$$

Upon making the following substitution for the concentration difference, $\Delta = c_2 - c_1$, the time dependent behavior for Δ can be expressed as an exponential [11]:

$$\Delta = \Delta_o \exp \left[\frac{-AD_b}{L} \left(\frac{1}{v_1} + \frac{1}{v_2} \right) t \right] \quad (11)$$

The quantity Δ_o is the concentration difference at the onset of a constant gradient.

The formation factor is estimated from the diffusion data through the use of a computer program that simulates the diffusion experiment by implementing the electro-diffusion equation. A similar computer program has been described previously [12]. The computer program performs an electro-diffusion transport calculation using Eqn. 5 and knowledge of the sample porosity and the pore solution chemistry. The microstructural diffusion coefficient D_μ is calculated from the formation factor using Eqn. 9. The formation factor is an independent input parameter that is varied until the calculated output of the computer program matches the experimental data.

The computer program calculated the solution to Eqn. 5 using a finite difference scheme. The system was represented by a one-dimensional mesh composed of 21 nodes. The differencing algorithm was fully explicit, but the stability criterion was satisfied by a factor of

five. The computer program calculated the activity coefficients using an implementation of the Pitzer equations [13] that was based on the PHRQPITZ [14] computer program. The diffusion potential was calculated using the local electro-neutral (zero current) hypothesis [6]. For the species flux \mathbf{j}_i , as given in Eqn. 5, the total current \mathbf{I}_T is the sum over the individual fluxes, each proportional to the species charge z_i :

$$\mathbf{I}_T = \sum_i z_i \mathbf{j}_i = 0 \quad (12)$$

The diffusion potential gradient is chosen so that this relation is satisfied at the boundary of each computational element, assuring both local and global charge neutrality.

Table 2: Comparison of diffusion coefficients D from the computer program (CP) and handbook (HB) values for some 1:1 valence salts. The handbook values are from the CRC Handbook of Chemistry and Physics.

Salt	conc. mol·L ⁻¹	D_{HB} 10 ⁻⁹ m ² ·s ⁻¹	D_{CP} 10 ⁻⁹ m ² ·s ⁻¹
KCl	0.01	1.917	1.902
	0.10	1.844	1.807
	1.00	1.892	1.801
NaCl	0.01	1.545	1.539
	0.10	1.483	1.476
	1.00	1.484	1.571
KI	0.10	1.865	1.829
	1.00	2.065	1.911

As a test of the computer program, the diffusion coefficient of 1:1 valence salts in bulk liquid are calculated by the computer program (CP) and the values compared to values reported in chemistry handbooks (HB) [15] values; the computer program was executed with both the formation factor and the porosity fixed at a value of one. The calculations are performed over a range of salt concentrations and the results are shown in Table 2. Generally, the computed results agree quite favorably with reported values, with the worst case being a difference of approximately 10 %.

Based on Eqn. 11, a semi-logarithmic plot of Δ versus time data should be a straight line. The slope of this line is determined first for the experimental data. To determine the formation factor \mathcal{F} from these data, values for \mathcal{F} are input to the computer program and are varied until a plot of the calculated values of Δ versus time, on a semi-logarithmic plot, has the same slope as the corresponding experimental data.

4 Results

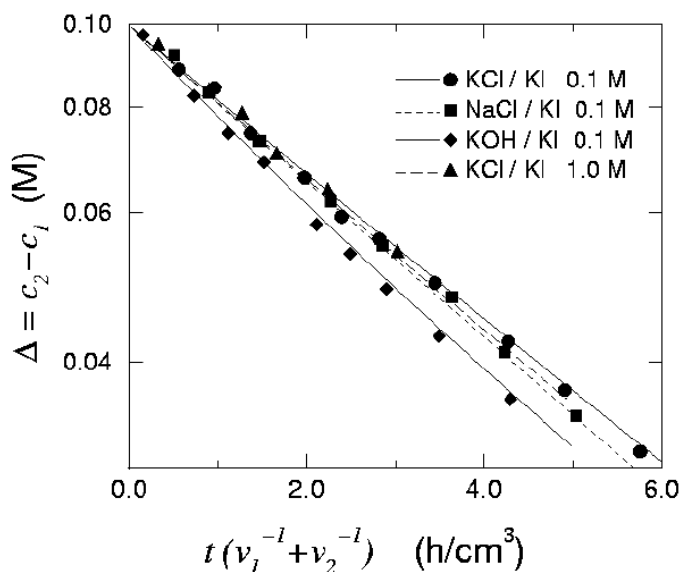


Figure 3: Concentration difference across each sample as a function of time. The experimental values are shown as filled symbols, the calculated values are shown as solid curves. The measurement uncertainties would appear as the same size as the symbols, so are omitted for visual clarity. The value of Δ for the 1.0 mol/L KCl system is divided by ten in order to appear on the same scale as the other data.

The measured values of Δ for the iodide concentration are shown as symbols in Fig. 3. The estimated uncertainties are approximately the size of the symbols, and are not shown as error bars for reasons of visual clarity. The KCl and the NaCl systems behaved similarly; the values of Δ for the 1.0 mol/L KCl system were divided by ten so that they could be

included on the same plot. The 1.0 mol/L KCl solution has a similar behavior to the 0.1 mol/L KCl system because the self diffusion coefficient D_∞ for K^+ , Cl^- , and I^- are nearly equal to one another. The estimated diffusion potential for both of the KCl systems was less than 1 mV, and was less than 5 mV for the NaCl system. The KOH system showed a marked difference in behavior. One reason for this is that the self diffusion coefficient D_∞ for OH^- is significantly greater than that of the other ions present, resulting in a calculated diffusion potential of approximately 16 mV.

Table 3: The values for the slope (AD_b/L) of the experimental data shown in Fig. 3. Also shown is the ratio D_∞/D_b , using D_∞ for iodide. The uncertainties shown for the slopes are the estimated standard deviation reported by the statistical software, and also characterize the uncertainty in the ratio D_∞/D_b reported.

System	AD_b/L ($cm^3 \cdot h^{-1}$)	D_∞/D_b
KCl – 0.1 mol/L	0.2004 ± 0.0032	11.1
NaCl – 0.1 mol/L	0.2118 ± 0.0032	10.3
KOH – 0.1 mol/L	0.2381 ± 0.0047	9.3
KCl – 1.0 mol/L	0.2079 ± 0.0050	10.7

The measured slopes of the experimental data, on semi-logarithmic axes, are shown in Table 3. The estimated standard deviations shown are typically less than 3 % of the slope value, suggesting that the constant gradient assumption is valid for these systems. In fact, the systems reached a constant gradient state at a relatively early age. The output from the computer program suggests that the constant gradient condition is achieved in less than 12 h.

Also shown in Table 3 are the values for the ratio D_∞/D_b , using the iodide value for D_∞ ($2.045 \times 10^{-5} \text{ cm}^2 \text{ s}^{-1}$ [5]). This ratio represents an incorrect application of using the formation factor to determine the apparent bulk diffusion coefficient. Since the quantity D_∞ in this ratio is a constant, the ratios are simply proportional to the apparent bulk

diffusivity D_b . However, this ratio does not reflect the actual formation factor, because the iodide self diffusion coefficient within the pore solutions is not equal to D_∞ . Also, it is clear that arbitrary changes in the pore solution will lead to changes in the apparent bulk diffusion coefficient of iodide in these systems, while the formation factor is nearly equal for all systems.

The correct values of the formation factor \mathcal{F} were determined from the experimental data using the aforementioned computer program, and are shown in Table 4, labelled \mathcal{F}_{sim} . Also shown in the table are the values of the formation factor calculated from the impedance spectroscopy measurements, labelled \mathcal{F}_{IS} . The uncertainty in \mathcal{F}_{IS} reflects the variation in the dc resistance measurement as mentioned previously. The values of \mathcal{F}_{sim} shown in Table 4 were used to calculate values for Δ , and these values of Δ are plotted in Fig. 3, denoted by the lines. The experimental data and the calculated values for the KCl and the NaCl systems were all nearly linear. The values of Δ for the KOH system are easily distinguished from the other systems.

The calculated values of \mathcal{F}_{sim} shown in Table 4 were consistent with the measured values \mathcal{F}_{IS} . The values of \mathcal{F}_{sim} varied by approximately 7 %, compared to the 18 % variation in the values of D_∞/D_b . The differences between the values of \mathcal{F}_{sim} and \mathcal{F}_{IS} were less than 3 % for the KCl and the NaCl system, and less than 8 % for the KOH system.

The calculated values \mathcal{F}_{sim} were generally greater than the measured \mathcal{F}_{IS} values. A partial explanation for this can be found in the data in Table 2. In that table, the estimated diffusion coefficients were consistently greater than the handbook values. This suggests that the computer program calculates an agglomerated diffusion coefficient that is larger than it is in reality. Therefore, for the computer program to agree with experimental data, the formation factor \mathcal{F}_{sim} must be made *greater* than its true value, which is consistent with the data in Table 4.

Sighting along the KOH data reveals that these data have some curvature. It is interesting

to note that the computed output (solid curve) also exhibits this nonlinear behavior. This suggests that this nonlinear behavior is due to effects of the pore solution chemistry since output from the computer program indicates that the iodide concentration profile across the sample is stable within 12 h. However, the calculated concentration profile of iodide is not linear due to the diffusion potential.

Table 4: Measured and calculated formation factors from impedance spectroscopy (F_{IS}), computer simulation (F_{sim}), and apparent diffusivity (D_∞/D_b) using D_∞ for iodide.

System	\mathcal{F}_{IS}	\mathcal{F}_{sim}	D_∞/D_b
KCl – 0.1 mol/L	10.7 ± 0.2	10.9	11.1
NaCl – 0.1 mol/L	10.9 ± 0.2	11.2	10.5
KOH – 0.1 mol/L	10.6 ± 0.2	11.4	9.3
KCl – 1.0 mol/L	10.7 ± 0.2	10.6	10.7

This electro-chemical effect of the KOH system is revealed in Table 4. The apparent diffusion coefficient of iodide in this system is considerably greater than that for the other systems. However, the computer calculation reveals that the required formation factor \mathcal{F}_{sim} is comparable to the values for the other test solutions. This fact demonstrates the effect of using the apparent diffusion coefficient D_b to characterize a microstructure. For that particular test solution, the apparent diffusion coefficient describes how the iodide ion behaves in the presence of KOH, but does not characterize its behavior in the presence of other test solutions. Similarly, it does not necessarily characterize how other ions behave in the same, or similar, microstructure.

Since the pore solution of cementitious systems is typically alkaline, the results for the KOH system have direct relevance to the prediction of ion transport in portland cement systems. The pore solution ionic strength in cementitious systems can be nearly ten times greater than the 0.1 mol/L KOH system studied here. Further, there will be number of additional ions present, with a corresponding number of self diffusion coefficients. This

raises the question of the correct method for characterizing the microstructure of these systems. Either predicting the formation factor from diffusion data or predicting the diffusion coefficient from a formation factor measurement will require a knowledge of the pore solution chemistry. For a formation factor measurement that implements pore solution extraction, a chemical analysis of the extracted pore fluid would be a logical extension of the measurement procedure. However, diffusion measurements typically do not reveal the chemical makeup of the pore solution, and so further experimentation may be required for experimental programs based upon diffusion measurements to characterize the microstructure of pore cementitious systems.

5 Conclusion

Experiments performed using ceramic frits yield evidence for the equivalence between the formation factor and the *microstructural* diffusion coefficient, which is a characterization of the porous microstructure. Due to the complexity of accounting for the chemical behavior of the pore solution, extracting the microstructural diffusion coefficient from diffusion data requires a numerical calculation. While the apparent diffusion coefficient depended upon the chemical makeup of the pore solution, the procedure outlined here was able to extract the microstructural diffusion coefficient for each system, yielding a similar value for the systems studied. The presence of KOH in the pore solution had a noticeable affect on the apparent diffusion coefficient of iodide. Due to the similarity between the self diffusion coefficient of iodide and chloride, one would expect similar effects on chloride ions in cementitious systems. The ability to extract the microstructural diffusion coefficient from observed data has a direct influence on service life modeling that can independently account for changes in either the pore structure or the pore solution chemistry. This is particularly important in cementitious systems containing pore solutions with large ionic strengths.

Acknowledgements

The author is grateful to Prof. Raymond A. Cook of the University of New Hampshire for performing the mercury intrusion porosimetry measurements. The author would like to acknowledge the partial support of the Nuclear Regulatory Commission for this work.

The author is also greatly indebted to Prof. Jacques Marchand of Université Laval for his guidance, discussions, and suggestions, and to Dr. James Beaudoin of the National Research Council (CANADA) for stimulating discussions.

References

- [1] See any of the conference proceedings such as Nilsson, L.O. and Ollivier, J.P. (eds.), ‘Chloride Penetration into Concrete,’ (RILEM, 1997).
- [2] Collins, R.E., ‘Flow of Fluids Through Porous Materials,’ (Reinhold Publishing, 1961).
- [3] Bockris, J.O’M. and Reddy, A.K.N., ‘Modern Electrochemistry,’ Volume 1, Plenum Press, 1970.
- [4] Snyder, K.A., Ferraris, C., Martys, N.S. and Garboczi, E.J., ‘Using impedance spectroscopy to assess the viability of the rapid chloride test for determining concrete conductivity,’ *J. Res. NIST* **105** (2000) 497–509.
- [5] Mills, R. and Lobo, V.M.M., ‘Self-Diffusion in Electrolyte Solutions,’ Elsevier, New York, 1989.
- [6] Rubinstein, I, ‘Electro-Diffusion of Ions,’ Society for Industrial and Applied Mathematics, Philadelphia, 1990.
- [7] Crank, J., ‘The Mathematics of Diffusion,’ (Oxford University Press, 1975).

- [8] Torquato, S., ‘Random heterogeneous media: Microstructure and improved bounds on effective properties,’ *Appl. Mech. Rev.* **44** (1991) 37–76.
- [9] Settle, F.A. (ed.), ‘Handbook of Instrumental Techniques for Analytical Chemistry,’ (Prentice Hall, 1997).
- [10] Schwartz, L.M., Sen, P.N., and Johnson, D.L., ‘Influence of rough surfaces on electrolytic conduction in porous media,’ *Phys. Rev. B* **40** (1989) 2450–2458.
- [11] Tyrrell, H.J.V. and Harris, K.R., ‘Diffusion in Liquids,’ (Butterworths, 1984).
- [12] Samson, E., Marchand, J., Robert, J.-L., and Bournazel, J.-P., ‘Modelling ion diffusion mechanisms in porous media,’ *Int. J. Numer. Meth. Engin.* **46** (1999) 2043–2060.
- [13] Pitzer, K.S., ‘Thermodynamics of electrolytes. I. Theoretical basis and general equations,’ *J. Phys. Chem.* **77** (1973) 268–277.
- [14] Plummer, L.N., Parkhurst, D.L., Fleming, G.W., and Dunkle, S.A., ‘A Computer Program Incorporating Pitzer’s Equations For Calculation of Geochemical Reactions In Brines,’ U.S. Geological Survey Report 88-4153, Reston, VA 1988.
- [15] Weast, R.C. (ed.), ‘CRC Handbook of Chemistry and Physics,’ (CRC Press, 1982).